SINTEF

On the mechanisms of consumption of calcium lignosulfonate by cement paste

Colombo, A., Geiker, M., Justnes, H., Lauten, R. A., & De Weerdt, K.

ON THE MECHANISMS OF CONSUMPTION OF CALCIUM LIGNOSULFONATE BY CEMENT PASTE

A. Colombo (1), M. Geiker (1), H. Justnes (1,2), R. A. Lauten (4), K. De Weerdt (1)

(1) Department of Structural Engineering, Norwegian University of Science and Technology, Norway

(2) SINTEF Building and Infrastructure, Trondheim, Norway

(3) Borregaard, Sarpsborg, Norway

ABSTRACT

The aim of this paper is to assess the mechanisms of consumption of softwood calcium lignosulfonate (LSs) by cement paste. The LSs consumption by two different cements (CX and ANL) and two reference materials ($CaCO_3$ and $Ca(OH)_2$) was investigated, either by adding the LSs immediately with the mixing water (IA) or after 10 minutes of hydration (DA). For IA, the increase in LSs dosage caused additional ettringite formation and an increase in particle surface area. This was not observed for DA. Since no AFm phase could be detected, intercalation in AFm seemed not to occur for the investigated materials. The main mechanism of LSs consumption for CX cement (both for IA and DA) and for ANL cement (only for DA) appeared to be monolayer adsorption. For IA, the amount of consumed LSs could not be ascribed exclusively to monolayer surface adsorption and other LSs consumption mechanisms might play a role.

1. INTRODUCTION

Water-reducers, or plasticizers, are commonly used as admixture for concrete. Their addition to fresh concrete allows obtaining highly fluid concrete at low water-binder ratios, improving the mechanical properties of the hardened concrete. To optimize the polymer-cement combination and the amount of admixture needed to achieve the desired workability, it is important to understand the mechanisms of consumption of plasticizer by cement paste.

24   The plasticizer investigated in this paper is a low-sugar softwood calcium lignosulfonate (LSs),

25   commonly used in concrete in the dosage of 0.25-0.40 mass % of binder. Lignosulfonates are

26   polyelectrolytes derived from lignins from pulping industry. The lignins are fragmented and

27   sulfonated, thereby becoming water-soluble. Lignin can be derived both from softwood and hardwood

28   trees, which results in lignosulfonates with different molecular weight and amount of molecular

29   functional groups (carboxyl groups, phenolic-OH, sulfonic groups). Lignosulfonate is known to have

30   medium retarding effect on cement hydration. The sugars naturally contained in lignin remain in

31   lignosulfonate after its production. These sugars contribute to longer setting times of cement, in

32   particular the hexoses, which can be removed by fermentation in low-sugar lignosulfonates. However,

33   studies in literature found that also sugar-free lignosulfonates exhibited pronounced retardation of

34   cement paste hydration, e.g. [1, 2].

35   Plasticizers interact with unhydrated and hydrated cement grains, as summarized in a recent literature

36   review by Marchon and Flatt [3]. In this paper, the amount of polymer uptaken by the cement paste is

37   defined as "consumed" as opposed to the free one dissolved in the pore solution. The mechanisms of

38   polymer consumption will be separately discussed in this paragraph.

39   The dispersing effectiveness of a superplasticizer on cementitious materials is, amongst others, a

40   function of its degree of adsorption on the surface of cement grains and hydrates. The adsorbed

41   plasticizer layer renders the total particle surface negatively charged, i.e. with a negative zeta potential.

42   As negatively charged particles approach each other there will be an electrostatic repulsion preventing

43   them from forming agglomerates. Additionally, when two surfaces approach enough for their adsorbed

44   layers to overlap, a steric force develops. This will contribute in hindering particles to get close

45   enough to form agglomerates. The key parameters that govern the steric repulsion are the adsorption

46   layer thickness and its conformation at the solid liquid interface [4].

47   The polymer will not be adsorbed equally on the four main cement phases. According to Yoshioka et

48   al. [5], much higher adsorption occurs on aluminate and ferrite than on the silicate phases. The amount

49   of adsorbed polymer on ettringite was found to be the largest amongst the cement hydrates by Zingg et

50   al. [6]. It must be noted that, in both the cited references, the results were reported by unit of mass and

51   not by unit of specific surface.

52   Polymer adsorption can also take place in multiple layers on cement particles and hydrates. After ideal

53   monolayer coverage, the cement particles will have a negative surface charge. Ca^{2+} ions will then be

54   electrostatically attracted to the negatively charged groups of the polymer and they will bond with

55   them. This Ca^{2+} outer layer will allow the adsorption of a further layer of negatively charged polymer

56   [7, 8], facilitating additional consumption of polymers.

57   Adsorption onto the surface of cement particles and hydrates is not the only potential consumption

58   mechanism taking place when a plasticizer is added to a cementitious system. Part of the water-

59   reducing admixture might also be intercalated in the hydration products, mainly in the layered

60   structure of AFm, and part of the admixture will remain dissolved in the aqueous phase, according to,

61   amongst others, [9-12]. When tricalcium aluminate (C_3A) enters in contact with water, it reacts

62   immediately forming, in absence of gypsum, the metastable layered phases C_4AH_{19} and C_2AH_8. In

63   presence of gypsum, C_3A will react with water forming $C_6A\bar{S}_3H_{32}$ (ettringite) and $C_4A\bar{S}H_{12}$

64   (monosulphate). C_4AH_{19}, C_2AH_8 and $C_4A\bar{S}H_{12}$ belong to the group of layered double hydroxides

65   (LDHs). Several anions and polyelectrolytes can intercalate in between the cationic layers of LDH

66   compounds by replacing their hydroxyl ions. According to Plank et al. [10], intercalation was found to

67   be possible for polymers with different structure, namely, linear, comb-like and polymer brushes with

68   very long side chains. The polymer intercalated in LDHs will no longer be available for dispersing

69   cement particles; therefore a higher dosage of polymer will be necessary to reach the desired

70   workability.

71   Another possible mechanism of polymer-cement interaction is complexation between functional

72   groups of the plasticizer and calcium ions dissolved in the pore solution, as observed in several studies

73   [13-16]. Collins et al. [13] found that calcium ions dissolved in a calcium lignosulfonate solution with

74   pH over 10-11 can hold together a matrix of lignosulfonate molecules, forming a gel. Other cations,

75   e.g. aluminium and iron, could also tightly bind to LS molecules. As mentioned by Sowoidnich et al.

76   [15], the interaction between calcium ions and polymer functional groups (mainly sulfonic and

77   carboxyl groups) can be divided into complexation of calcium ions in aqueous solution, complexation

78   of calcium ions on particles surface (adsorption) and formation of polymer-containing clusters.

79   Formation of Ca-polymer complexes will increase the amount of consumed polymer if they are

80   precipitated or form colloids that are filtered away when collecting pore solution, and decrease the

81   amount of free Ca^{2+} ions in the pore solution, lowering the Ca-Si ratio of the pore solution, hence

82   possibly modifying the hydration reactions and the resulting hydrates, as stated by Yousuf et al. [17].

83   The polymer molecules captured in the complexes with calcium ions might still have some free

84   anionic functional groups on their outer regions. These anionic functional groups might as well be

85   attracted to the positive charged calcium ions adsorbed on the polymer layer over cement particles and

86   hydrates. The calcium-polymer complexes might then bind to the cement particles already covered

87   with polymer, decreasing the amount of free LSs in the pore solution and forming multiple layers of

88   polymer adsorbed. For this reason the mechanisms of calcium complexation and multilayer adsorption

89   can be considered interrelated and, sometimes, undistinguishable from each other.

90   The subject of this paper is to investigate the mechanisms consuming a low-sugar softwood calcium

91   lignosulfonate (LSs) in paste of two Portland cements with different surface area and C_3A content. The

92   effects were studied both by adding the lignosulfonate immediately with the mixing water (IA) and by

93   adding it after 10 minutes of hydration (DA). The amount of polymer consumed by the cement paste

94   was determined by UV-spectrometry and adsorption isotherms were calculated. Comparison of

95   adsorption isotherms onto cement and reference materials representative of cement but which do not

96   hydrate ($CaCO_3$ and $Ca(OH)_2$), allow a better elucidation of the LSs consumption mechanisms in

97   simpler systems than cement. Changes in the surface area of the hydrated cement particles were

98   investigated by BET. The changes in composition and amount of cement hydrates caused by the

99   addition of lignosulfonate were investigated with thermogravimetric analysis (TGA).

2. EXPERIMENTAL

2.1 Materials

The mechanisms of plasticizer consumption by cement paste were studied adding a low-sugar softwood calcium lignosulfonate (LSs) to two Portland cements: a CEM I 52.5 N (ANL) and a CEM I 52.5 R (CX). The two cements were chosen because of their different surface area and C_3A content. The content of the main clinker phases of the cements quantified by XRD Rietveld are given in Table 1. The chemical composition of the cements and the loss of ignition at 950 ºC determined by XRF are reported in Table 2. The particle size distribution (d_{10}, d_{50}, d_{90}), Blaine surface area and density, BET surface area are given in Table 3.

A sugar-reduced softwood calcium lignosulfonate (LSs) was used as plasticizer. Its mass weighted molecular weight (M_w), as measured with gel permeation chromatography (GPC), was 29000 g/mol and the number weighted molecular weight (M_n) was 2100 g/mol, giving broad molar-mass dispersity ($Đ_M$) equal to 13.8. The molar-mass dispersity, also called polydispersity index, is defined as the ratio between M_w and M_n [18]. Additional physical and chemical properties of the lignosulfonate are listed in Table 4. For the lignosulfonate used in the present investigation, the sugars were removed from the polymer molecule by fermentation and resulting alcohol by distillation. The LSs was dissolved in deionised water to concentrations varying from 1 to 45 % to ease dosing, and the water content was included in the calculation of the water-to-binder ratio (w/b).

$CaCO_3$ and technical-grade precipitated $Ca(OH)_2$ were also mixed with lignosulfonate in order to study some simplified model systems. Their specific surface areas determined by BET are reported in Table 5. In order to mimic the basic pH of cement paste, these samples were mixed with LSs solution diluted in artificial pore water. The artificial pore water was a solution of NaOH and KOH with K/Na molar ratio equal to 2 and measured pH of 12.9.

123 **2.2 Sample preparation**

124 **2.2.1 Portland cements**

125 Cement was mixed with distilled water and/or lignosulfonate solution in a high-shear mixer MR530 by

126 Braun at intensity 6 obtaining pastes with w/b = 0.4. About 200 ml of cement paste was mixed per

127 batch. In order to investigate the effect of the time of addition of lignosulfonate, two different mixing

128 procedures were compared: immediate addition of LSs with the mixing water (IA) and delayed

129 addition of LSs at 10 minutes of hydration (DA).

130 For IA, the binder was mixed with distilled water (and/or lignosulfonate diluted in distilled water or

131 artificial pore water) according to the procedure used by Vikan [19]: 30 seconds mixing and scraping

132 the walls of the mixer to homogenize the mix, 5 minutes resting and 1 minute mixing.

133 For DA, the binder and 85% of the needed water were mixed according to the following mixing

134 procedure: 30 seconds mixing and scraping the mixer walls to homogenize the mix, 10 min resting

135 (delay time chosen according several studies in literature [20-23]). LSs and the remaining 15% of the

136 needed water were then added to the mix which was mixed for 1 minute.

137 After mixing, about 35 ml of paste was poured in 50 ml sealed plastic centrifuge tubes and let rest

138 until the chosen analysis time.

139 **2.2.2 Calcium carbonate**

140 Calcium carbonate has been shown to be a suitable model system for investigating stability and

141 rheology of cement paste. Mikanovic et al. [24] showed that calcium carbonate exhibits colloidal

142 properties very similar to those of cement paste at early ages (hydration < 1 hour). $CaCO_3$ exhibit

143 surface properties and flocculation behavior similar to that of cement paste, namely, an irregular

144 spheroid shape, and a low surface charge in water. In addition it has a very low solubility, also at high

145 pH. In addition, this material was expected not to noticeably react with water.

146 About 300 g of $CaCO_3$ was mixed with about 90 g of LSs solution dissolved in artificial pore water in

147 a high-shear mixer MR530 by Braun at intensity 6. The mixing procedure was identical to the one

148   used for neat cement with IA. The water-solid ratio by mass was 0.3. Several LSs dosages were

149   analysed, as reported in Table 6. The samples were let to rest for 30 minutes prior to being analysed.

150   **2.2.3 Calcium hydroxide**

151     $Ca(OH)_2$ is one of the main cement hydrates and its solubility is about 100 times higher than the one of

152     $CaCO_3$, so it appears to be useful to investigate the possible interaction between the LSs and calcium

153   ions. About 5 g of $Ca(OH)_2$ was mixed with about 40 g of LSs solution dissolved in artificial pore

154   water in plastic centrifuge tubes and mixed by hand for 1 minute. The high fineness of the $Ca(OH)_2$

155   powder required a water-solid ratio by mass of 8.0. The mixing solution contained increasing amounts

156   of LSs, as reported in Table 6. All the samples were let to rest for 30 minutes prior to being analysed.

157   **2.3 Methods**

158   **2.3.1 Adsorption isotherms**

159   Polymer adsorption by a solid is usually described through isotherms, in which the amount of polymer

160   adsorbed is plotted against the total amount of polymer added to the system [25]. The shape of an

161   isotherm is largely determined by the adsorption mechanism. In this study, the isotherms were drawn

162   relating the amount of LSs consumed by the cement paste to the amount of total LSs added to the

163   sample.

164   With the help of a calibration curve, achieved by measuring the UV absorbance of pure LSs solutions

165   in artificial pore water at different concentrations, the amount of free plasticizer (g LS/100 g solution)

166   was calculated. This amount was related to the amount of binder in the sample (g LS/100 g binder).

167   The LSs consumed by the investigated systems was then calculated by subtracting the amount of free

168   LSs from the total amount of LSs initially added to the sample, as displayed in the following equation:

169   consumed LSs = total LSs – free LSs   (1)

170   The absorbance of the pore solution was measured with UV-spectroscopy. In order to confirm the

171   results obtained with UV-spectroscopy, the adsorption isotherm of ANL cement for IA was measured

172   also with total organic carbon analysis (TOC). Potential removal of polymer aggregates by filtration

173   was eliminated as error source, by comparing TOC analysis of filtered and un-filtered samples which

174   were found to be very similar

175   **2.3.1.1 UV-spectroscopy**

176   UV-spectrometry allowed measuring the absorbance of the pore solution at increasing LSs dosage.

177   The LSs dosages tested are summarized in Table 6.

178   The pore solution was extracted from the cement paste by centrifuging the samples in a Heraeus

179   Megafuge 8 centrifuge by Thermo Scientific for 3 minutes at the speed of 4500 rpm. The supernatant

180   pore solution was extracted and filtered with 0.45 μm cellulose acetate syringe filters by VWR. The

181   amount of free LSs in the pore water was measured with UV-spectrometry with a Genesys 10S UV-

182   spectrophotometer by Thermo Scientific. Several wavelengths have been reported in literature to study

183   the amount of lignosulfonate in pore solution: Perche [26] and Ratinac [27] used 280 nm, Uchikawa et

184   al. [28] and Houst at al. [4] used 284 nm, Vikan [19] used 283 nm. Samples diluted 1:100 with

185   distilled water were scanned with different wavelengths from 190 to 300 nm using distilled water as

186   blank reference sample. For the plasticizer used in this study, 281 nm was chosen as the best

187   wavelength to measure the absorbance value.

188   The amount of plasticizer consumed by cement paste as a function of increasing hydration time was

189   determined by centrifugation of pastes aged for different times (5-120 minutes). As displayed in

190   Figure 1, it was found that at 10 minutes of hydration the LSs uptake reached an equilibrium value. All

191   the samples were then analysed aftert 30 minutes of hydration.

192   **2.3.1.2 Total organic carbon (TOC)**

193   The concentration of free polymer in the pore solution extracted by ANL cement (0.2; 0.4; 0.8; 1.0;

194   1.5 mass % of binder LSs IA) was measured with the total organic carbon analysis (TOC). The TOC

195   analysis was performed using a Vario TOC Cube by Elementar. The extracted pore solution was

196   filtered with 0.20 μm cellulose acetate filters. Part of the sample was acidified with 2 drops of

197   concentrated HCl to prevent any formation of precipitates in the solution. The amount of consumed

198   LSs was measured by TOC on the same sample before and after acidification. Acidification did not

199   lead to any variation in the results. No notable difference in the results obtained with UV-spectroscopy

200   and with TOC was displayed up to a LSs dosage of 0.6 mass % of binder. Over this dosage, the

201   consumed LSs from TOC measurements was from 3 to 15 % higher than the one measured with UV-

202   spectroscopy. The difference might be due to the differences in sample preparation (different sample

203   dilution, different filter used) and the measurement techniques. However, the results obtained with the

204   two different techniques showed similar trends.

205   **2.3.2 Solvent exchange**

206   A solvent exchange procedure with isopropanol was used to stop the hydration of the cement paste

207   after 30 minutes of hydration. The samples were then analysed with thermogravimetric analysis

208   (TGA) and BET.

209   About 5 ml of cement paste was transferred in a 50 ml centrifuge tube and centrifuged for 1 minute at

210   2000 rpm. The supernatant water was removed. About 40 ml of isopropanol was poured in the

211   centrifuge tube. The tube was shaken for 30 seconds and let to rest for 5 minutes. The sample was

212   centrifuged again for 1 minute at 2000 rpm and the supernatant liquid was removed. The solvent

213   exchange procedure with isopropanol was repeated once, followed by a final solvent exchange with 10

214   ml of petroleum ether. The resulting paste was let to dry for 2 days in a desiccator over silica gel, and

215   soda lime to minimize carbonation. After drying, the samples were homogenized in a porcelain mortar

216   and stored in sealed containers in a desiccator over silica gel and soda lime until analysis.

217   **2.3.3 Thermogravimetric analysis (TGA)**

218   The thermogravimetric analysis (TGA) was performed with a Mettler Toledo TGA DSC3+ on

219   hydrated cement paste after stopping the hydration using solvent exchange. Approximately 200 mg of

220   cement paste powder was loaded in 600 μl alumina crucibles. The samples were heated from 40 to

221   900°C at a rate of 10°C/min while purging with 50 ml/min N_2.

222   **2.3.4 Characterization of surface area of hydrated cement pastes by BET**

223   The BET measurements were performed using a Tristar II Plus by Micromeritics on samples of which

224   the hydration was stopped with the solvent exchange procedure. Before the measurement, the samples

225   were degassed for about 5 minutes at room temperature. The measurement was performed purging the

226   samples with nitrogen at room temperature, which took about 10 minutes. The sample mass was about

227   2 g. The samples did not undergo any thermal treatment before the measurement to avoid any possible

228   destruction of ettringite, as recommended by Mantellato et al. [29, 30].

3 RESULTS

3.1 Adsorption isotherms

231   The adsorption isotherms of ANL and CX cement pastes, $CaCO_3$, and $Ca(OH)_2$ were obtained by

232   measuring the amount of consumed polymer for an increasing dosage of polymer in the mix as

233   described in Table 6. Higher LSs dosages were used for $Ca(OH)_2$ due to its very small particle size,

234   and thus larger specific surface. For CX cement it was not possible to extract pore water at LSs

235   dosages over 1.0 mass % of binder due to paste hardening after 30 minutes of hydration. The LSs was

236   added to the cement paste either immediately with the mixing water (IA), or after 10 minutes of

237   hydration (DA). The results are presented as consumed LS per mass % of binder in Figure 2a, and per

238   m^2 of unhydrated substrate surface area available for adsorption in Figure 2b. The isotherms were

239   obtained by fitting the experimental data to the non-linear Langmuir model, according to the equation

240   described by Marchon et al. [31]: $$m_{SA} = \frac{m_{SA}^{\infty} K c_A}{1 + K c_A} \tag{2}$$

241   Where m_{SA} is the adsorbed mass, m_{SA}^{∞} is the adsorbed mass at the plateau, K is a chemical equilibrium

242   constant, and c_A is the concentration in solution.

243   As reported in [31], the Langmuir model is not ideal for a system like cement paste, which surface

244   area changes with hydration and where the polymer is not adsorbed equally on all cement phases. In

245   addition, in the present paper, the Langmuir equation was used to fit results plotted as amount of

246   consumed polymer versus dosage of added polymer, rather than versus the equilibrium concentration

247   of polymer remaining in solution. Therefore, its K-value does not bear any physical meaning, and the

248   fit can only be considered as a visual guide for the eye.

249   The adsorption isotherm of $Ca(OH)_2$ is omitted in Figure 2 a because of the higher LSs dosages used.

250   It must be noted that the water-solid ratio by mass was 0.3 for $CaCO_3$ and 8.0 for $Ca(OH)_2$, while it

251   was 0.4 for the neat cements.

252   The results were also presented in Figure 3 as consumed LSs amount (% of the LSs amount added)

253   versus the LSs amount added. Figure 3 shows that all the adsorption isotherms for the cements

254   displayed similar LSs consumption at low LSs dosage (up to about 0.25 mass % of binder LSs). At

255   these low LSs dosages, about 75 % of the LSs added was consumed both for IA and for DA. At LSs

256   dosages higher than about 0.25 mass % of binder, the curves obtained for IA showed a LSs

257   consumption of about 70 % of the LSs added. The consumption kept constant with increasing LSs

258   dosages. For DA, the amount of LSs consumed decreased from about 75 % to about 30 % of the LSs

259   added when the LSs dosage increased from 0.25 to 1.5 mass % of binder.

260   As displayed in Figure 2, for IA, no adsorption plateau could be detected within the tested range,

261   neither for ANL nor for CX cement. This has also been observed by others, e.g. by Vikan [19] and

262   Ratinac et el. [27]. The isotherms' shape indicated a continuous LSs uptake when more LSs was added

263   to the mix.

264   For DA, an adsorption plateau was found for both cements. The isotherms that reached an adsorption

265   plateau also displayed a considerably lower amount of LSs consumed by the cement pastes compared

266   to those that did not reach any plateau.

267   **3.2   Surface area of hydrated cement particles**

268   The BET surface area was measured for ANL and CX cement pastes with increasing LSs amounts

269   hydrated for 30 minutes. The hydration was stopped by solvent exchange after 30 minutes. The results

270   and their linear fit are shown in Figure 5.

271   For both cements the surface area after 30 minutes of hydration was found to increase as the dosage of

272   plasticizer added to the cement paste increased. The increase in surface area was remarkably larger for

273   CX than for ANL cement, and for IA compared to DA.

11

274   New adsorption isotherms were calculated dividing the amount of consumed LSs by the actual surface

275   area of ANL and CX cements after 30 minutes of hydration as measured with BET for both IA and

276   DA. The isotherms were obtained by fitting the experimental data to the non-linear Langmuir model,

277   as described in paragraph 3.1. The results are displayed in Figure 6. For CX cement, the isotherms

278   obtained with IA and DA nearly coincide, both reaching an adsorption plateau. On the contrary, for

279   ANL cement, even when expressed relative to the hydrated surface area, the adsorption isotherms

280   remain qualitatively similar to those obtained considering the unhydrated surface area.

281   **3.3   LSs molecular footprint**

282   As displayed in Figure 6, for ANL cement, the adsorption plateau was reached for a total LSs amount

283   between 0.8 and 1.2 mass % of binder, which the authors assume to be due to the achievement of

284   monolayer surface coverage. The amount of LSs consumed at the achievement of the plateau was

285   considered equal to the value m_{SA}^{∞} obtained with a non-linear regression analysis based on equation 2.

286   Knowing the molecular weight of the LSs molecule (29000 g/mol) and the specific surface area of

287   hydrated ANL cement as measured with BET (174 m^2/100g cement with 0.8 mass % of binder LSs,

288   and 184 m^2/100g cement with 1.2 mass % of binder LSs), it is possible to calculate the LSs "molecular

289   footprint". The error connected to the molecular footprint was calculated considering an estimated

290   error or 30% for the measurement of the surface area with BET and of the LSs molecular weight, and

291   the standard error of m_{SA}^{∞}. The LSs molecular footprint resulted to be about 20 ± 10 nm^2 for ANL

292   cement for both LSs dosages, which mostly agrees to the data given by the producer for the same LSs

293   (50 ± 30 nm^2). The producer calculated this value from the plateau values of the adsorption isotherms

294   of LSs on MgO at alkaline pH.

295   For CX cement, the adsorption plateau was reached for a total LSs amount between 1.2 and 1.5 mass

296   % of binder. Knowing the specific surface area of hydrated CX cement as measured with BET (286

297   m^2/100g cement with 1.2 mass % of binder LSs, and 301 m^2/100g cement with 1.5 mass % of binder

298   LSs), the LSs molecular footprint was calculated as about 20 ± 10 nm^2 for both LSs dosages. This

299   value is equal to the one obtained for ANL cement.

300 In order to get a deeper understanding of the actual plasticizer consumption mechanisms by cement

301 paste, the adsorption isotherms determined with ANL or CX cements were compared to those obtained

302 for simplified model systems, $CaCO_3$ and $Ca(OH)_2$.

303 The $CaCO_3$ isotherm is displayed in Figure 2 a per mass % of dry powder. The $CaCO_3$ isotherm

304 reached an adsorption plateau for a total LSs amount between 0.2 and 0.4 mass % of binder. At

305 surface saturation, about 0.06 g of admixture was adsorbed on 100 g of $CaCO_3$. Since the specific

306 surface area of the unhydrated $CaCO_3$ was measured with BET as 57 m^2/100g, the surface coverage

307 can be calculated as about 920 m^2/g $_{LS}$. Hence, the molecular "footprint" (coverage) of LSs was

308 calculated as about 60 ± 30 nm^2 for both LSs dosages. This result partly agrees with the data given by

309 the producer (50 ± 30 nm^2).

310 The $Ca(OH)_2$ isotherm, omitted in the figures due to the high LSs dosages used, reached an adsorption

311 plateau for a total LSs amount between 8.0 and 12.0 mass % of binder. The high LSs dosages at which

312 the plateau is reached is most likely due to the high specific surface area of the $Ca(OH)_2$ particles. At

313 surface saturation, about 0.06 g of admixture was adsorbed on 100 g of $Ca(OH)_2$. Since the specific

314 surface area of the unhydrated $Ca(OH)_2$ was measured with BET as 1666 m^2/100g, the molecular

315 "footprint" of LSs was calculated as about 40 ± 20 nm^2 for both LSs dosages. This value resulted lower

316 than the one obtained for $CaCO_3$, still being included in the range given by the producer (50 ± 30

317 nm^2).

318 The consumed LSs at plateau achievement and the molecular footprint calculated for the different

319 materials can be found in Table 7. It has to be kept in mind that the LSs has a broad polydispersity

320 index, which leads to a wide error in the molecular footprint given by the producer. The results

321 reported in Table 7 showed that a relatively similar footprint was obtained for the model materials, i.e.

322 $CaCO_3$ and $Ca(OH)_2$, and the real cements.

323

324 **3.4   Hydrates characterization**

325   In order to investigate the effects of LSs on hydrates formation, thermogravimetric curves were

326   measured on ANL and CX cement pastes with 1.5 mass % of binder LSs added with IA and DA. A

327   reference sample of ANL and CX pastes without LSs was also measured. The hydration of the tested

328   samples was stopped after 30 minutes with the solvent exchange procedure using isopropanol and

329   petroleum ether, as described in paragraph 2.3.2. The results are displayed in Figure 4 a, b.

330   Several peaks could be observed. According to Lotenbach et al. [32], amongst others, the peak at

331   about 120 ℃ and the smaller one at 240 ℃ indicate the presence of ettringite (ettr.). The peak around

332   160 ℃ represents the decomposition of sulfates. The sulfates will be most likely gypsum (x = 2) for

333   ANL cement. CX cement originally contains anhydrite (x = 0), which will not show any peak in the

334   TGA curve, since it does not contain water, and hemihydrate (x = 0.5). After 30 minutes of hydration,

335   hemihydrate will be partly or completely converted to gypsum. The peak around 160 ℃ in CX cement

336   will then be due to the decomposition of gypsum and/or hemihydrate. The peak around 420 ℃ shows

337   the presence of portlandite (CH); the ones around 610 ℃ and 780 ℃ represent the decomposition of

338   carbonates (CO_2). The peaks over 500 ℃ can be attributed both to the decomposition of limestone

339   included in the used cements and, for the samples containing LSs, to the decomposition of LSs. No

340   peak ascribable to AFm phases was detected.

341   The results show that, for IA, the addition of LSs led to additional formation of ettringite and reduced

342   amount of gypsum. For DA, in presence of LSs, no remarkable changes in the ettringite or gypsum

343   amounts were observed. The LSs addition caused an increase in the weight loss in the carbonate

344   region both for IA and DA. Similar trends were observed for both cements, even though remarkably

345   more ettringite and fewer sulfates were measured for CX cement, which might be linked to the larger

346   amount of C_3A in CX cement than in ANL cement.

347

4 DISCUSSION

The subject of this paper is to investigate the mechanisms consuming LSs in paste for two Portland cements, both for immediate and delayed addition of plasticizer. From literature the potential main mechanisms are: polymer intercalation into early cement hydrates; surface multilayer adsorption / complexation between functional groups of the plasticizer and calcium ions dissolved in cement pore solution; and monolayer surface adsorption of LSs on cement particles and hydrates. Each mechanism will be discussed separately in the following section.

4.1 Mechanisms of polymer consumption by the cement paste

4.1.1 Intercalation

According to, amongst others, Flatt and Houst [9], intercalation in AFm is generally considered to be the main cause of the difference between the adsorption isotherms obtained for IA or for DA. According to the theory, from the moment cement enters in contact with water, calcium aluminates start being consumed in AFt formation. In order for polymer intercalation to take place, calcium aluminates and polymer must be simultaneously available in solution. In case of DA, most hydrated aluminates have already been consumed in AFt formation at the time the polymer is added, hence the aluminates will no longer be available to form intercalated AFm.

Zingg et al. [6] formulated an alternative explanation for the difference in polymer consumption between IA and DA, which does not include intercalation. They hypothesized that, for IA, due to the dispersive effect of the plasticizer, numerous fine ettringite particles are floating in the pore solution, providing additional particle surface area for adsorption. On the contrary, with DA, the ettringite particles have already precipitated on the C_3S surface and cannot be redispersed. Hence, there will be no increase in surface area and, consequently, in polymer adsorption. However, it must be kept in mind that Zingg et al. did not investigate the amount of surface of ettringite which is made available through a change of the initial hydration reactions by the addition of the polymer.

The adsorption isotherms presented in Figure 2a,b displayed a remarkable difference in LSs consumption between the isotherm obtained for IA and the one obtained for DA. However, no peak

374 corresponding to AFm phase could be detected with TGA, as shown in Figure 4a,b. For the materials

375 investigated in this paper, intercalation in AFm seems less likely as a LSs consumption mechanism for

376 the investigated materials and dosages, while the theory of Zingg et al. [6] appears more feasible.

377 4.1.2 Calcium complexation / multilayer surface adsorption

378 In the case that LSs would be consumed in calcium complexes, either in solution or as multilayer

379 surface adsorption, the adsorption isotherms would display an increase in LSs consumption with the

380 amount of total LSs added, even for LSs dosages over the surface saturation value, as calcium is

381 buffered by the cement hydration.

382 In this study, the adsorption isotherms of both $CaCO_3$ and $Ca(OH)_2$ reached an adsorption plateau, as

383 shown in Figure 2 b. According to Lide [33], $CaCO_3$ has a solubility of 0.0014 g/100g in cold water,

384 while $Ca(OH)_2$ of 0.185 g/100g. Because of the negligible release of calcium ions by $CaCO_3$, calcium

385 complexation or multilayer adsorption with LSs molecules would be limited. The solubility of

386 $Ca(OH)_2$ is about 100 times higher than the one of $CaCO_3$. However, also for $Ca(OH)_2$ no calcium

387 complexation or multilayer adsorption with LSs molecules seemed to take place. Therefore, the LSs

388 consumed by both $CaCO_3$ and $Ca(OH)_2$ was most likely entirely due to monolayer adsorption of LSs

389 molecules on the particles surface.

390 Concerning the two cements, as shown in Figure 2a,b, the isotherm for both ANL and CX cement

391 reached an adsorption plateau for DA. As for $CaCO_3$, the main LSs consumption seems to be

392 monolayer surface adsorption. For IA, on the contrary, the isotherm of both the cements did not reach

393 an adsorption plateau, indicating a continuous polymer uptake by the cement paste the more polymer

394 is added. However, the authors assume that, as calcium complexation/multilayer adsorption was minor

395 or not existing for both $CaCO_3$ and $Ca(OH)_2$, and for the cements in case of DA, also for the cements

396 in case of IA calcium complexation/multilayer adsorption should not be a major mechanism behind

397 the LSs consumption.

16

4.1.3 Monolayer surface adsorption

In the case that LSs would adsorb as a monolayer onto the cement particles, the adsorption isotherms would display a plateau when the entire surface is covered by the polymer, as displayed in several studies [5, 19, 34, 35]. This mechanism, monolayer adsorption, can be described by the Langmuir model [31]. Since such a plateau is reached by both ANL and CX cements when the polymer was added with DA, and considering the above conjectures, it is likely that monolayer surface adsorption is the main mechanism of LSs consumption for DA.

No adsorption plateau was reached when the polymer was added with IA. This might be due to different reasons. First, it is possible that the increase in LSs consumption solely occurs due to the increase in particle surface area available for adsorption due to cement hydration, as displayed in Figure 5. In this case, the only mechanism of LSs consumption would be monolayer surface adsorption. Another possibility is that other consumption mechanisms were acting in addition to surface adsorption. In order to examine these possibilities, it is first necessary to further investigate the effect of the increase of particle surface area with hydration on LSs consumption by the cement paste.

4.2   The effect of LSs on the increase in particle surface area with hydration

As displayed in Figure 5, the BET measurements showed an increase in particle surface area with hydration, which was influenced both by the plasticizer dosage and by its addition time. The increase in surface area was larger for CX than for ANL cement, and greatly larger for IA than for DA for both cements. As shown in Figure 6, the influence of the different surface area of the two hydrated cements could be eliminated by expressing the results relative to the surface area of the hydrated substrate as measured with BET.

For CX cement, the isotherms obtained with IA and DA nearly coincide, both reaching an adsorption plateau. This indicates that the higher LSs consumption by CX cement paste measured with IA is mainly due to the larger increase in particle surface area that takes place with IA, which, on the contrary, does not take place with DA. Hence, for CX cement, the main mechanism for LSs consumption seems to be monolayer surface adsorption for both IA and DA.

424 Regarding ANL cement, even when expressed relative to the hydrated surface area, the adsorption

425 isotherms remain qualitatively similar to those obtained considering the unhydrated surface area.

426 Therefore, for ANL cement, monolayer surface adsorption does not seem to be the only LSs

427 consumption mechanism for IA.

428 Finally, as displayed in Figure 4, when LSs was added to the cement pastes with IA, a higher amount

429 of ettringite was formed by both cements compared to the sample without LSs. Moreover, as shown in

430 Figure 5, the LSs addition led to an increase in particle surface area. The increase was larger for CX

431 cement, which also presented a larger amount of ettringite. Therefore, the increase in particle surface

432 area seems to be directly correlated to the increased amount of ettringite produced by the cements in

433 presence of LSs.

434 **5   SUMMARY AND CONCLUSIONS**

435 The aim of this paper is to obtain a better understanding of the mechanisms for lignosulfonate (LSs)

436 consumption by cement paste. This is considered to be crucial to maximize the efficiency of the

437 plasticizer. According to literature, the mechanisms behind the consumption of a softwood low-sugar

438 calcium lignosulfonate can potentially be: monolayer adsorption, intercalation, and calcium

439 complexation/multilayer adsorption. The LSs consumption by two different cements at immediate (IA)

440 and delayed (DA) addition was investigated using UV-spectroscopy and adsorption isotherms were

441 calculated. The changes in particle surface area with hydration were measured with BET. The changes

442 in hydrates due to the addition of LSs were examined with TGA. The results obtained for cement

443 pastes were compared to those obtained for reference materials (i.e. calcium carbonate, calcium

444 hydroxide). The following conclusions were drawn:

445 - The presence of LSs in the cement paste led to an additional formation of ettringite for IA,

446   while an increase was not detected for DA;

447 - An increase in LSs dosage led to an increase in particle surface area after 30 minutes of

448   hydration. This increase was considerably higher for IA rather than for DA.

449   -   Neither AFm nor intercalated AFm were observed. Therefore, intercalation cannot explain the

450   differences in LSs consumption observed between IA and DA.

451   -   The mechanism of LSs consumption seems to be mainly monolayer surface adsorption for CX

452   cement (both for IA and for DA), and for ANL cement when DA was applied. For ANL, other

453   mechanisms in addition to monolayer surface adsorption appear to play a role in LSs

454   consumption when IA is applied.

455 6   FUTURE RESEARCH

456 In a follow-up study, the effect of LSs on rheology, rate of hydration, and amount and morphology of

457 ettringite in pastes of the same cements will be investigated both for IA and DA. A deeper

458 investigation on the mechanisms behind LSs consumption in ANL cement for IA will also be

459 considered for future research.

460 7   ACKNOWLEDGEMENTS

467 8   REFERENCES

468 [1] V.S. Ramachandran, M.S. Lowery, Conduction calorimetric investigation of the effect of retarders
469 on the hydration of Portland cement, Thermochimica Acta, 195 (1992) 373-387.
470 [2] K. Reknes, J. Gustafsson, Effect of modifications of lignosulfonate on adsorption on cement and
471 fresh concrete properties, 7th International Conference on Superplasticizers and Other Chemical
472 Admixtures in Concrete, 2000, pp. 127-142.
473 [3] D. Marchon, R.J. Flatt, 12 - Impact of chemical admixtures on cement hydration, Science and
474 Technology of Concrete Admixtures, Woodhead Publishing2016, pp. 279-304.
475 [4] Y.F. Houst, P. Bowen, F. Perche, A. Kauppi, P. Borget, L. Galmiche, J.-F. Le Meins, F. Lafuma,
476 R.J. Flatt, I. Schober, P.F.G. Banfill, D.S. Swift, B.O. Myrvold, B.G. Petersen, K. Reknes, Design and

477 function of novel superplasticizers for more durable high performance concrete (superplast project),
478 Cement and Concrete Research, 38 (2008) 1197-1209.
479 [5] K. Yoshioka, E.-i. Tazawa, K. Kawai, T. Enohata, Adsorption characteristics of superplasticizers
480 on cement component minerals, Cement and Concrete Research, 32 (2002) 1507-1513.
481 [6] A. Zingg, F. Winnefeld, L. Holzer, J. Pakush, S. Becker, L. Gauckler, Adsorption of
482 polyelectrolytes and its influence on the rheology, zeta potential, and microstructure of various cement
483 and hydrate phases, Journal of Colloid and Interface Science, 323 (2008) 301-312.
484 [7] Y. Zhang, X. Kong, Correlations of the dispersing capability of NSF and PCE types of
485 superplasticizer and their impacts on cement hydration with the adsorption in fresh cement pastes,
486 Cement and Concrete Research, 69 (2015) 1-9.
487 [8] M.Y.A. Mollah, W.J. Adams, R. Schennach, D.L. Cocke, A review of
488 cement–superplasticizer interactions and their models, Advances in Cement Research, 2000,
489 pp. 153-161.
490 [9] R.J. Flatt, Y.F. Houst, A simplified view on chemical effects perturbing the action of
491 superplasticizers, Cement and Concrete Research, 31 (2001) 1169-1176.
492 [10] J. Plank, H. Keller, P.R. Andres, Z. Dai, Novel organo-mineral phases obtained by intercalation
493 of maleic anhydride–allyl ether copolymers into layered calcium aluminum hydrates, Inorganica
494 Chimica Acta, 359 (2006) 4901-4908.
495 [11] C. Jolicoeur, M.-A. Simard, Chemical admixture-cement interactions: Phenomenology and
496 physico-chemical concepts, Cement and Concrete Composites, 20 (1998) 87-101.
497 [12] C. Giraudeau, J.-B. D'Espinose De Lacaillerie, Z. Souguir, A. Nonat, R.J. Flatt, Surface and
498 intercalation chemistry of polycarboxylates copolymers in cementitious systems, Journal of the
499 American Ceramic Society, 92 (2009) 2471-2488.
500 [13] J.W. Collins, J.M. Torkelson, A.A. Webb, Some viscosity properties of lignosulfonates isolated
501 by ultrafiltration, Journal of Agricultural and Food Chemistry, 25 (1977) 743-746.
502 [14] J. Plank, B. Sachsenhauser, Experimental determination of the effective anionic charge density of
503 polycarboxylate superplasticizers in cement pore solution, Cement and Concrete Research, 39 (2009)
504 1-5.
505 [15] T. Sowoidnich, T. Rachowski, C. Rößler, A. Völkel, H.-M. Ludwig, Calcium complexation and
506 cluster formation as principal modes of action of polymers used as superplasticizer in cement systems,
507 Cement and Concrete Research, 73 (2015) 42-50.
508 [16] F. Caruso, S. Mantellato, M. Palacios, R.J. Flatt, ICP-OES method for the characterization of
509 cement pore solutions and their modification by polycarboxylate-based superplasticizers, Cement and
510 Concrete Research, (In review).
511 [17] M. Yousuf, A. Mollah, P. Palta, T.R. Hess, R.K. Vempati, D.L. Cocke, Chemical and physical
512 effects of sodium lignosulfonate superplasticizer on the hydration of portland cement and
513 solidification/stabilization consequences, Cement and Concrete Research, 25 (1995) 671-682.
514 [18] R.G. Gilbert, M. Hess, A.D. Jenkins, R.G. Jones, P. Kratochvil, R.F.T. Stepto, Dispesity in
515 polymer science, Pure applied chemistry, 81 (2009) 351-353.
516 [19] H. Vikan, Rheology and reactivity of cementitious binders with plasticizers, Department of
517 Materials Science and Engineering, NTNU Trondheim, 2005.
518 [20] J. Hot, Influence des polymères de type superplastifiants et agents entraineurs d'air sur la
519 viscosité macroscopique des matériaux cimentaires, Université Paris-Est, Paris, 2013.
520 [21] I. Aiad, Influence of time addition of superplasticizers on the rheological properties of fresh
521 cement pastes, Cement and Concrete Research, 33 (2003) 1229-1234.
522 [22] G. Chiocchio, A.E. Paolini, Optimum time for adding superplasticizer to Portland cement pastes,
523 Cement and Concrete Research, 15 (1985) 901-908.
524 [23] K.-C. Hsu, J.-J. Chiu, S.-D. Chen, Y.-C. Tseng, Effect of addition time of a superplasticizer on
525 cement adsorption and on concrete workability, Cement and Concrete Composites, 21 (1999) 425-430.
526 [24] N. Mikanovic, K. Khayat, M. Pagé, C. Jolicoeur, Aqueous CaCO3 dispersions as reference
527 systems for early-age cementitious materials, Colloids and Surfaces A: Physicochemical and
528 Engineering Aspects, 291 (2006) 202-211.
529 [25] P.C. Hiemenz, R. Rajagopalan, Principles of colloid and surface chemistry, Taylor & Francis
530 Group1997.

531 [26] F. Perche, Adsorption de Polycarboxylates et de Lignosulfonates sur Poudre modele et Ciments,
532 École Polytechnique Federale de Lausanne, 2004.
533 [27] K.R. Ratinac, O.C. Standard, P.J. Bryant, Lignosulfonate adsorption and stabilization of lead
534 zirconate titanate in aqueous suspension, Journal of Colloid and Interface Science, 273 (2004) 442-
535 454.
536 [28] H. Uchikawa, S. Hanehara, T. Shirasaka, D. Sawaki, Effect of admixture on hydration of cement,
537 adsorptive behaviour of admixture and fluidity and setting of fresh cement paste, Cement and
538 Concrete Research, 22 (1992) 1115-1129.
539 [29] S. Mantellato, M. Palacios, R.J. Flatt, Reliable specific surface area measurements on anhydrous
540 cements, Cement and Concrete Research, 67 (2015) 286-291.
541 [30] S. Mantellato, M. Palacios, R.J. Flatt, Impact of sample preparation on the specific surface area of
542 synthetic ettringite, Cement and Concrete Research, 86 (2016) 20-28.
543 [31] D. Marchon, S. Mantellato, A.B. Eberhardt, R.J. Flatt, 10 - Adsorption of chemical admixtures,
544 Science and Technology of Concrete Admixtures, Woodhead Publishing2016, pp. 219-256.
545 [32] B. Lothenbach, P. Durdzinski, K. De Weerdt, Thermogravimetric analysis, A Practical Guide to
546 Microstructural Analysis of Cementitious Materials, CRC press2015.
547 [33] D.R. Lide, Handbook of chemistry and physics, 72nd ed., CRC Press1991-1992.
548 [34] H. Bessaies-Bey, J. Hot, R. Baumann, N. Roussel, Consequeces of competitive adsorption
549 between polymers on the rheological bahaviour of cement pastes, Cement and Concrete Research,
550 (2014).
551 [35] R.J. Flatt, Interparticle forces and Superplasticizers in Cement Suspensions, École
552 Polythechnique Fédérale de Lausanne, 1999.

553

554 Notation

555 apw   artificial pore water

556 ANL   Anlegg cement

557 CX   Cemex cement

558 IA   immediate addition of plasticizer

559 DA   delayed addition of plasticizer

560 LSs   softwood low-sugar Ca-lignosulfonate

561 OPC   ordinary Portland cement

562 w/b   water-binder ratio

563 LDHs   layered double hydroxides

564

565 List of tables

577

578 List of figures

596

597 Table 1 – *Main phases in cement ANL and CX from XRD-Rietveld analysis performed at École des*

598 *Mines d'Alès, France. [a]: results obtained with TGA analysis*

Phase composition (%wt)	ANL	CX
Alite	60.5	54.3
Belite	14.2	18.8
Aluminate cubic	1.3	4.7
Aluminate ortho.	0.9	2.4
Ferrite	14.0	6.5
periclase	0.4	1.1
quartz	0.3	-
calcite	3.2/ 3.8 [a]	3.6/ 3.7 [a]
portlandite	1.1/ 1.4 [a]	2.6/ 2.5 [a]
anhydrite	-	2.1
hemihydrate	2.6	1.8
gypsum	1.0	-
arcanite		0.6
aphthitalite	0.4	0.7
thenardite	-	0.8

599

600 Table 2 – *Chemical composition of the raw materials given by the producers*

Chemical compound (%wt)	ANL	CX
Fe_2O_3	3.50	2.60
TiO_2	0.22	0.25
CaO	62.70	64.00
K_2O	0.40	1.00
P_2O_5	0.15	0.23
SiO_2	20.60	20.00
Al_2O_3	4.40	4.60
MgO	1.60	2.40
Na_2O	0.30	0.20
SO_3	3.30	3.60
LOI (%) 1000 °C	1.6	1.7
Sum	97.17	98.88

601

602　Table 3 - *Physical properties of ANL and CX cements performed at École des Mines d'Alès, France,*

603　*or given by the producer (*).*

	ANL	CX
Surface area (BET) (m^2/kg)	890	1326
Blaine surface (m^2/kg) *	360	540
Density (g/cm^3) *	3.13	3.09
d_{10} (μm)	2.0	2.0
d_{50}	12.0	10.0
d_{90}	34.0	26.0

604

605　Table 4 - *Chemical and physical properties of the lignosulfonate plasticizer used*

Plasticizer type	Mw	Org S ($\propto SO_3$)	SO_4^{2-} (mass %)	Ca^{2+}	Na	COOH	φ-OH	Total sugar (%)
LSs	29000	4.6	0.9	4.6	0.9	7.1	1.4	8.3

606

607　Table 5 – *Surface area (from BET) of CaCO$_3$ and Ca(OH)$_2$*

	CaCO$_3$	Ca(OH)$_2$
Surface area (BET) (m^2/kg)	570	16661

608

609　Table 6 – *Tested samples to obtain adsorption isotherms*

Material	LSs addition procedure	LSs dosage tested (mass % solid)
ANL cement	IA	0.1; 0.2; 0.4; 0.6; 0.8; 1.2; 1.5
	DA	0.05; 0.1; 0.25; 0.4; 0.8; 1.2; 1.5
CX cement	IA	0.1; 0.2; 0.4; 0.6; 0.8; 1.0
	DA	0.05; 0.1; 0.2; 0.4; 0.8; 1.2; 1.5
CaCO$_3$	IA	0.05; 0.1; 0.2; 0.4; 0.8; 1.0; 1.2; 1.5

| Ca(OH)$_2$ | IA | 1.0; 2.0; 5.0; 8.0; 12.0; 22.0 |

610

611 Table 7 – *Molecular footprints calculated for the different materials. * Equal to m_{SA}^{∞} in equation 2 ***

612 *The surface area used in the calculations was the hydrated one for the two cements and the*

613 *unhydrated one for the two model materials*

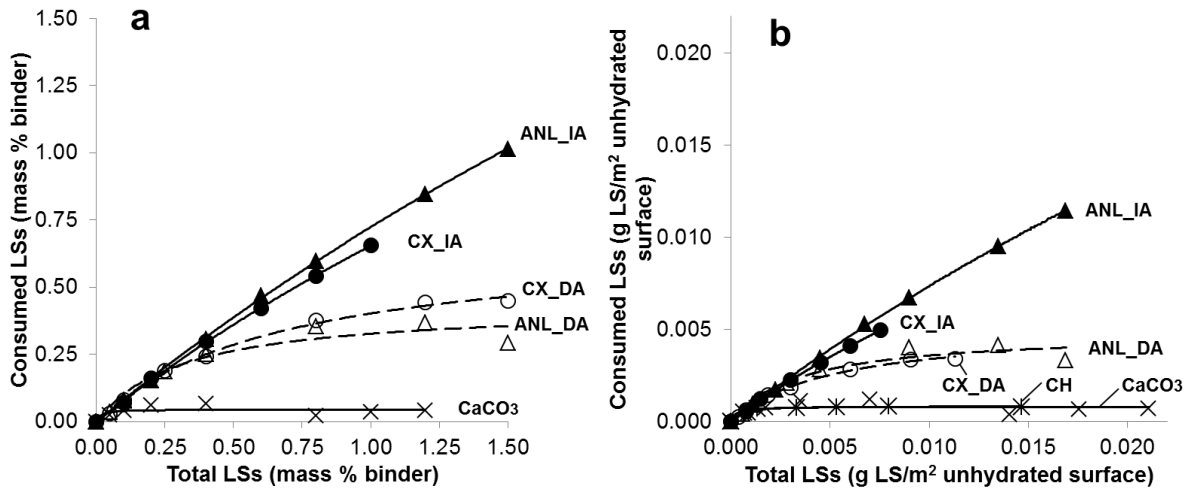| Material	Added LSs at plateau (mass % of binder)	Consumed LSs at plateau * (mass % of binder)	Molecular footprint ** (nm^2)
ANL cement	0.8 – 1.2	0.42 ± 0.05	20 ± 10
CX cement	1.2 – 1.5	0.68 ± 0.03	20 ± 10
CaCO$_3$	0.2 – 0.4	0.045 ± 0.009	60 ± 30
Ca(OH)$_2$	8.0 – 12.0	1.99 ± 0.31	40 ± 20

614
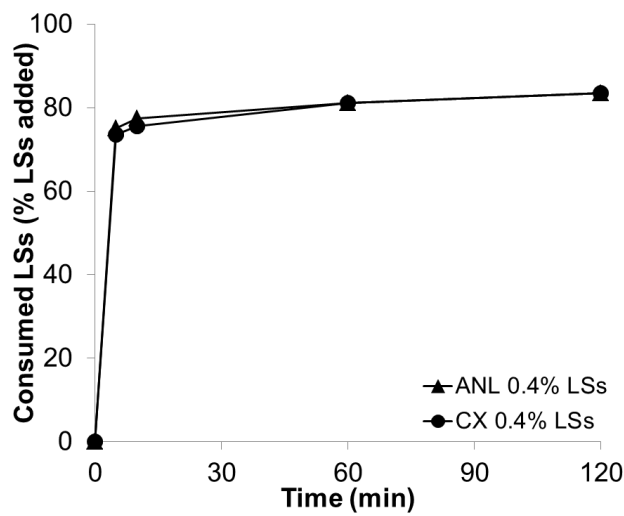
615

616 Figure 1 - *Amount of consumed LSs as % of added LSs vs. hydration time of ANL and CX cement*

617 *pastes with 0.40 mass % of binder LSs*

618

619   Figure 2a, b – *Amount of consumed LSs after 30 min. of hydration vs. amount of LSs added to neat*

620   *ANL and CX cements (IA and DA), and to CaCO₃*. The results are calculated per mass % of binder in*

621   *fig. 2 a and per unit of surface area available for adsorption of unhydrated particles in fig. 2 b. * In*

622   Figure 2*a, the isotherms of CH is omitted due to the higher LSs dosage used for this sample.*
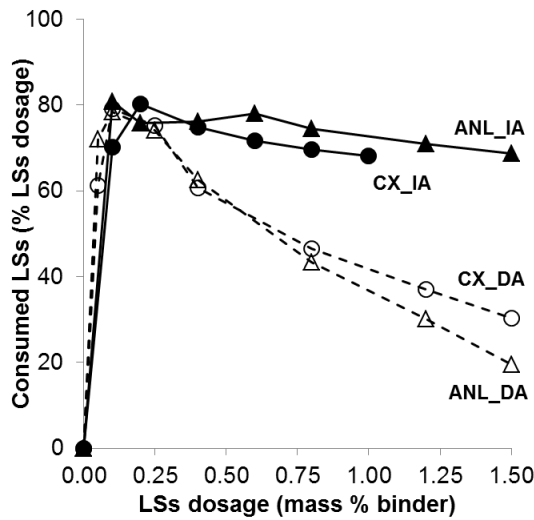
623

624   Figure 3 – *Consumed LSs (% LSs dosage) vs. LSs dosage (mass % of binder) for pastes of ANL and*

625   *CX cements where LSs was added both with IA and DA*

26

626
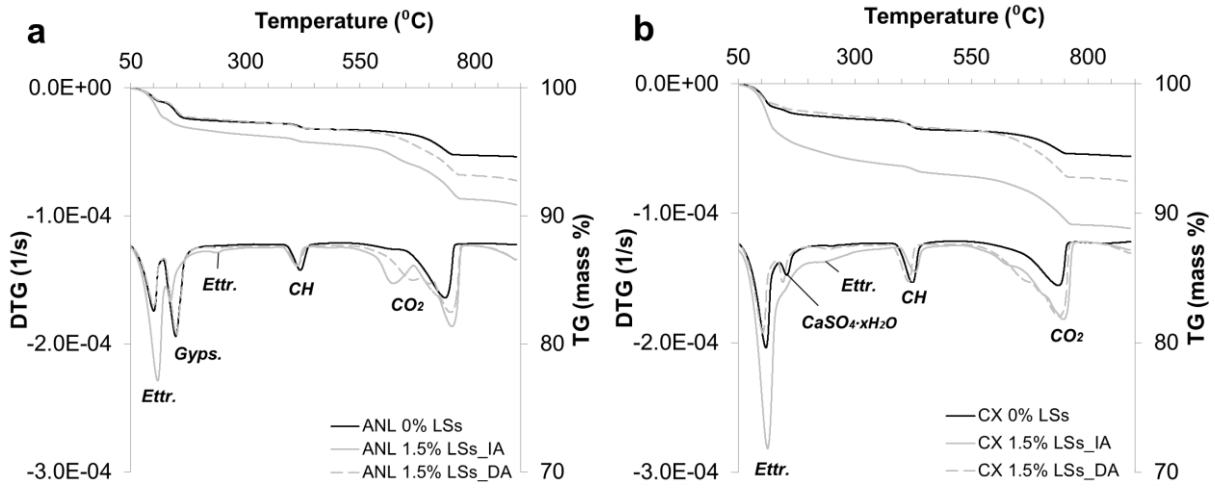
Figure 4 a, b - *Thermogravimetric curves and their derivatives for ANL (a) and CX (b) cement paste*

without LSs (black) and with 1.5 mass % of binder LSs (gray)(full line for IA and dotted line for DA)

for which hydration was stopped after 30 minutes. The peaks corresponding to the decomposition of

ettringite (ettr.), hemihydrate ($CaSO_4·0.5H_2O$) or gypsum ($CaSO_4·2H_2O$), portlandite (CH) and

carbonates (CO_2)

632
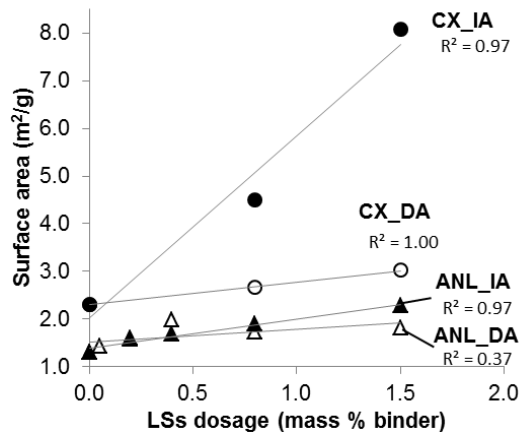
Figure 5 – *Surface area of ANL and CX cement particles hydrated for 30 min. both for IA and DA vs.*

the total dosage of LSs added (mass % of binder)

27

635
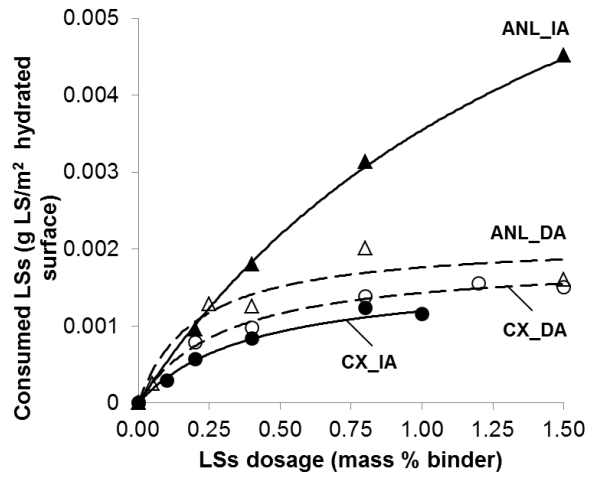
Figure 6 - A*mount of consumed LSs at 30 min. hydration (calculated as unit of surface area of*

637 *hydrated substrate) vs. amount of LSs added to neat ANL and CX cement (IA and DA) (calculated as*

638 *mass % of binder). For CX cement, the data points for 0.2; 0.4; 1.2 mass % of binder LSs (IA/DA)*

639 *were calculated with interpolation and were not experimentally measured*